Available online at www.sciencedirect.com

ScienceDirect

Procedia IUTAM 23 (2017) 138 – 146

Procedia IUTAM

www.elsevier.com/locate/procedia

IUTAM Symposium on Growing solids, Moscow, Russia (June 23 – 27, 2015)

Comparative Study of Selective Laser Melting and Direct Laser Metal Deposition of Ni_3Al Intermetallic Alloy

Dmitry Kotoban [a*], Aleksey Nazarov [a], Igor Shishkovsky [a, b]

[a] *Moscow State University of Technology 'STANKIN', Vadkovsky pereulok 3a, Moscow, 127055 Russia*
[b] *Lebedev Physical Institute (LPI) of Russian Academy of Sciences, Samara branch, Novo-Sadovaja st. 221, Samara, 443011 Russia*

Abstract

The Ni_3Al intermetallics involve more attention because of inherent material properties especially interesting in high temperature application. In this study, the Selective Laser Melting (SLM) and Direct Laser Metal Deposition (DLMD) are used to manufacture the single-tracks and layers. The optical microscopy, SEM, XRD and EDX microelement analysis were involved for the comparison of the methods. The materials showed no significant differences but each SLM and DLMD have the target application.

Peer-review under responsibility of the scientific committee of the IUTAM Symposium on Growing solids

Keywords: Selective Laser Melting ; SLM ; Laser Direct Metal Deposition ; DLMD ; Ni based superalloy ; NiAl intermetallic

1. Introduction

For the Additive Manufacturing (AM) the Selective Laser Melting (SLM) and Direct Laser Metal Deposition (DLMD) are the useful processes for the complex net shaped and near net shaped metal 3D parts producing [1]. Both methods provide significant freedom in design but several differences in the efforts for post-processing. Several researches were carried out to present the possibilities of AM with SLM and DMD [2, 3]. At present, the AM is sufficiently advanced to offer an industrial application allowing a new parts design, customization, functionality and performance in target area [4]. Taking into account the economics of the AM the methods of SLM and DMLD could be precisely attracted to aerospace, energy and automotive industries.

* Corresponding author. Tel.: +7-910-426-9543; Fax: +7-499-973-3152.
E-mail: d.kotoban@stankin.ru

Peer-review under responsibility of the scientific committee of the IUTAM Symposium on Growing solids
doi:10.1016/j.piutam.2017.06.014

The major phenomenon is taking place in both the SLM and DLMD processes is a laser-powder/substrate

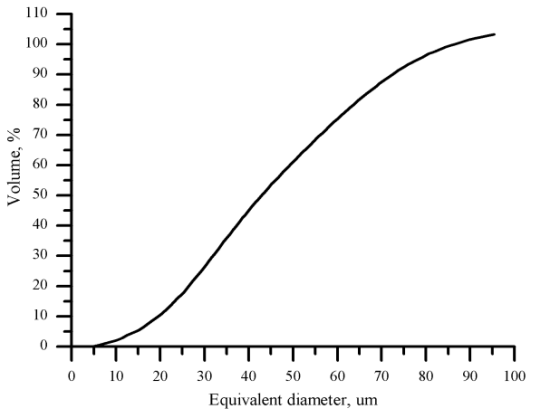

Figure 1. Granulometry of the Ni_3Al powder.

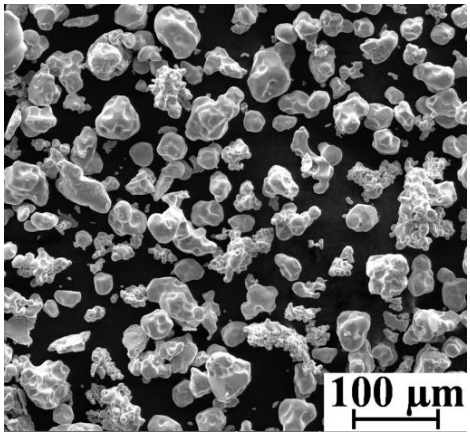

Figure 2. SEM images of Ni_3Al powder.

interaction that occurs under varying conditions. For the SLM process, the laser beam exposing the surface of powder spreaded on the powder bed while in the DMD powder the laser beam in flight irradiates particles. In this regard, the difference in single-track geometry, microstructures, elementary and phase composition are expected. Recently, the separate SLM and DLMS studies were performed, for example [5-7]. This study involves the SLM and DLMD to produce comparative data on the manufacturing of objects from Ni_3Al material.

At present, special attention is paid to the intermetallic alloys in consideration of their aerospace high-temperature applications for the parts manufacturing or as protective coatings. The nickel aluminides based on γ and (γ+γ') Ni_3Al phases have several advantages such as melting point of about 1385 °C, a low density (~ 7.53 g/cm^3), thermal stability up to melting, increase in the yield point up to 900 °C and a high heat resistance up to 1250 °C in atmosphere, flame, water and alkalis, weldability with steel and copper [8]. In addition, several studies investigate the Ni_3Al as a material with high abrasive wear, erosion and cavitation resistance [9-11]. In this regard, the Ni_3Al intermetallide could be proposed for turbojet nozzles, afterburner ducting parts and engine hot section blades.

Recently, Bazyleva et al. studied the casting of nickel aluminides and the properties after the heat treatment [12]. Cao et al. investigate the spark plasma sintering of Ni_3Al and the oxidation behavior [13]. Zhu et al. show the hot pressed structures of Ni_3Al with additions in order to investigate the high temperature tribological behavior [9]. Laser cladding, cold spraying and laser-aided self-propagating high-temperature synthesis of Ni_3Al were presented by Shishkovsky et al. [7, 14-16]. The plasma cladding was used to prepare the Ni_3Al by Zhang L.et al. [17].

In this paper, the SLM and DLMD were involved to produce 3D-objects of Ni_3Al intermetallics. The microstructures, elementary and phase composition, microhardness were studied in order to appreciate the technologies abilities and make comparison of the manufacturing processes.

2. Material and Methods

2.1. Materials

For the current study, the commercially available powder of pre-alloyed intermetallic Ni85Al15 was used (JSC Polema, Russia). The powder elementary composition was the stoichiometric composition of Ni_3Al phase. The powder producing method involves reducing with the help of calcium hydrides. A granulometry study made with help of the Alpaga 500 nano instrument (Occhio SA, Belgium) shows the statistical distribution of the particles by equivalent diameter of d_{10}= 30.7 µm, d_{50}= 46.8 µm, d_{90}= 65.0 µm with a mean equivalent diameter about 35 µm. The distribution is showed on fig. 1. Powder presents an irregular morphology that was identified by the SEM

investigation using Tescan Vega 3 LMH instrument (the Czech Republic) (fig. 2). The EDX analysis shows nearly

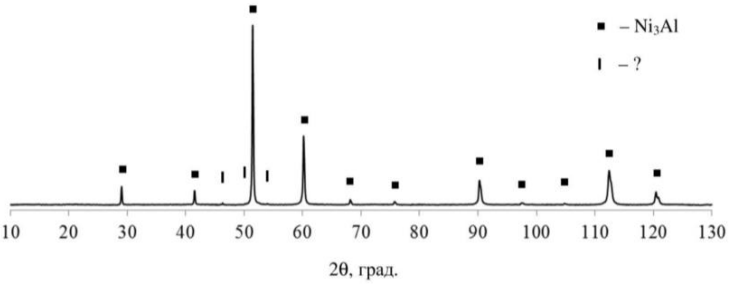

Figure 3. Powder X-ray diffraction pattern.

specified by manufacturer elementary composition. In the X-ray analysis on XRD Empyrean (Panalytical, Netherlands), it was showed one-phase composition of Ni_3Al with traces of unidentifiable secondary phase (fig. 3), apparently, as a result of powder manufacturing method. For the experiments, the powder was sieved, blended and dehumidified by heating at the temperature of 100 °C within 4 hours. The carbon steel St20 was used as a substrate.

2.2. Experimental Methods

A laboratory design pilot unit was used for the SLM process. The machine contains the continuous-wave Ytterbium fiber laser source of 200 W (1075 nm wavelength) of maximum power (IPG Photonics, Russia), the galvanometer with F-theta lens, the powder delivering system and movable platforms. The processing error of the movable systems was about 20 μm. The SLM laboratory setup provides argon shielding during the technological process. The powder was deposited on the technological platform with powder levelling system and the laser beam was computer controlled to scan the powder bed surface.

During the experiments, the main technological parameters were varied in order to investigate the process parameters influence on the microstructure and geometry of the single track. In this regard, the laser power was 50 W – 150 W, the range of scanning speed was 10-240 mm/s and the proposed layer thickness was constant of about 80 (±5) μm. The focused laser spot was about 70 μm with focusing distance of 420 mm. After the process parameter optimization, the multilayer objects were produced. The hatching distance between the tracks in layer was about 70 μm.

For the DLMD study, the 3D CNC machine Trucell 3008 (Trumpf, Germany) was used. The energy source was the Yb:YAG disc laser of 2kW maximum output power with a wavelength of 1030 nm. The machine is equipped with the coaxial laser cladding head and the 2-channel powder feeding system. The powder was supplied in the working zone through the nozzle with the aid of the argon shielding gas as well as the carrying gas (helium) at the rate of 10 and 15 l/min, respectively. The positioning accuracy of the relative displacement was about 30 μm.

During the experiments, the laser power varied within a range of 80-400 W, the scanning speed was 50-600 mm/min (0.83-10 mm/s) and the powder feeding rate was 3.8-9 g/min. Series of single tracks was produced for process parameters optimization as well as the multilayered objects with track overlaps (the hatching distance was 100 μm and the layer depth was 200 μm) with optimal parameters. The laser spot diameter was constant of 200 μm on the 7 mm standoff distance of the nozzle; the focusing distance was 200 mm.

2.3. Microstructural CHARACTERIZATION

Metallographic specimens were prepared following the standard procedure. The samples were subjected to the etching with acetic acid: HNO_3 : HCl solution in volume ratio 10:10:15 and $CuSO_4$ + HCl + H_2O solution in volume ratio 20cc : 20cc : 4g (Marble's reagent) to reveal a general structure. Metallographic analysis were made with help of the optical microscope Olympus BX51 (Japan) and the SEM in order to investigate the macrostructure health and

to compare the microstructure characteristics. The composition of the samples was determined by EDX/SEM as well as the phase analysis was carried out with X-ray diffractometer DRON-3 (Russia) with Co - K_α radiation. Hardness analysis was performed on Vickers hardness tester PMT-3M (Russia) at load of 100g.

3. Results and Discussions

3.1. Side View of the Surfaces and Process Parameters

The simplest unit produced by the SLM and DLMD is the single track. Primarily, the geometry of the tracks is provided by the kinetics of the powder consolidation in the laser exposure zone with a tremendous influence of processing parameters. During the experiments, the optimization of parameters was carried out with producing a number of tracks. The track geometries for the SLM and DLMD are similar (representation of Gaussian transversal energy distribution in the laser beam) but the minimum track width for SLM process was 100 μm while for DLMD it was about 200 μm (fig. 4a,b, 5a). Figures 4b and 5c (arrows show the manufacturing direction) show the top surface of the SLM and DLMD layers that represents more smooth SLM surface. Instead, the DLMD shows process that is more versatile especially in build-up rates terms. Figure 4c shows the one-layered objects (fig. 4c, left side) and two-layered objects (fig. 4c, right side) produced with different powder feeding rate (3 g/min (top side) and 9 g/min (bottom side)) with the post-laser treatment in order to improve the surface conditions. It is clear that the SLM provides more accurate objects with better surface conditions but the DLMD shows more flexibility. Both processes are presented layered structure with a repetition of 100…200 μm (fig. 4b and 5c). This phenomenon is referenced to the hatching distance and tracks overlapping in the layer.

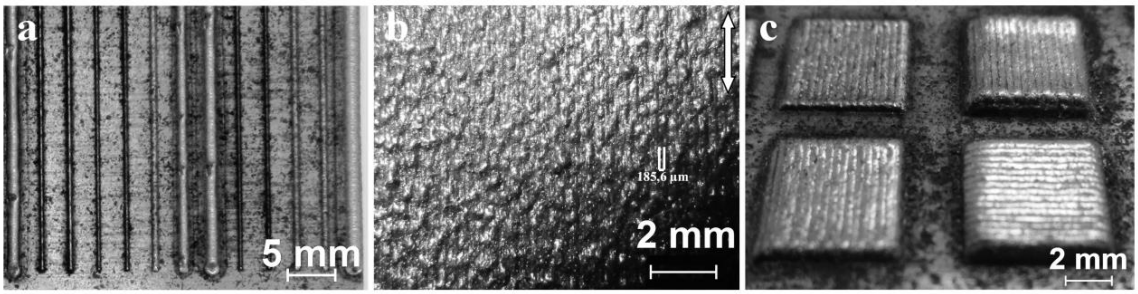

Figure 4. Primitive objects manufactured with the DLMD: a) single tracks, b, c) top surfaces of layers.

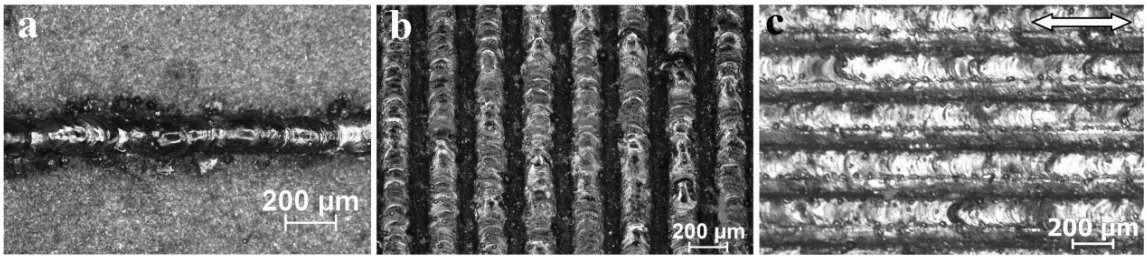

Figure 5. Primitive objects manufactured with the SLM: a) single track, b) single tracks set, c) top surface of a layer.

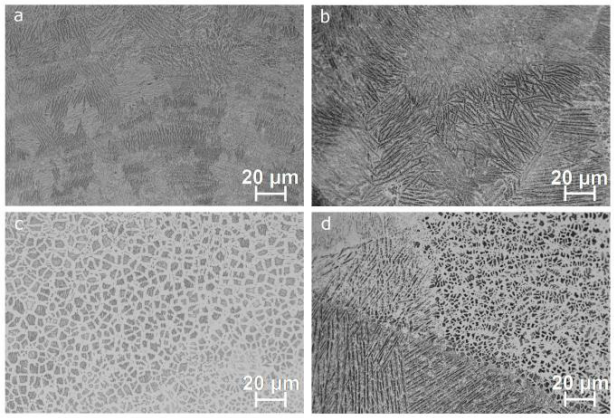

Figure 6. Optical micrographs of the DLMD-produced (a, c) and the SLM-produced (b, d) samples: a, b – perpendicular to the laser beam scanning direction, c, d – parallel to the laser beam scanning direction.

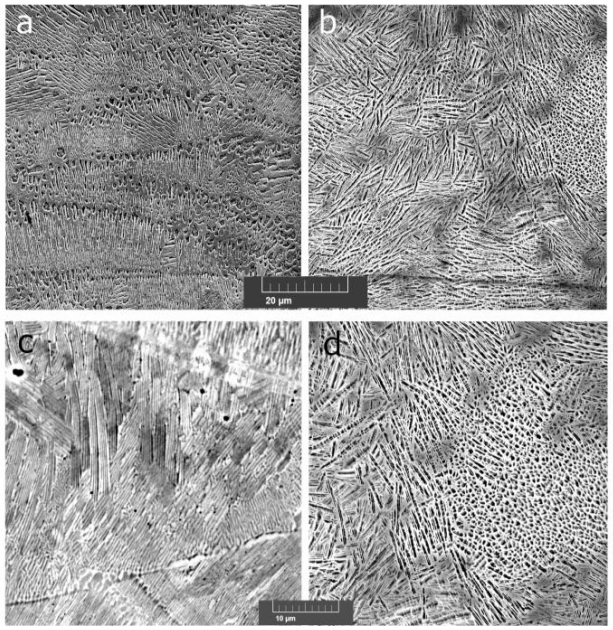

Figure 7. SEM micrographs of the DLMD-produced (a, c) and the SLM-produced (b, d) samples.

3.2. Microstructures

The microstructure of the specimens shows the directional solidification and elongation for both processes (fig. 6). The samples present two types of microstructures: perpendicular (fig. 6 a, b) and parallel (fig. 6 c, d) to the laser beam scanning direction that is directly influenced by scanning speed, i.e. melting/solidification conditions. The dendrites growing perpendicular to the laser beam scanning direction show almost similar measurements: dendrite characteristic branches forms 1.5…2.0 µm, dendrites length of 10…20 µm and a grains size of 25…40 µm.

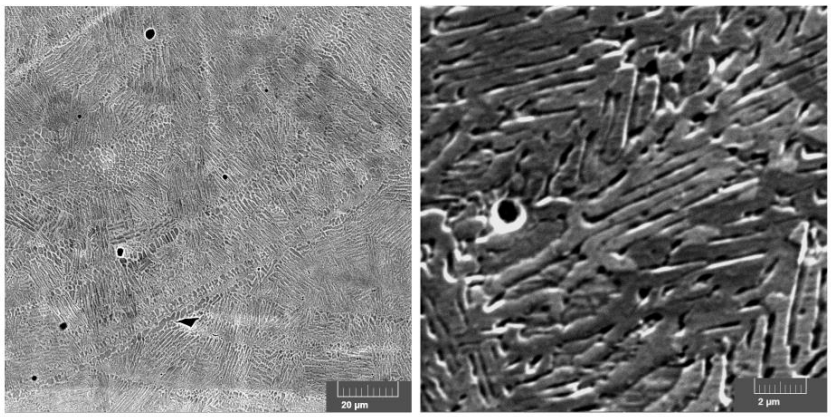

Figure 8. Generic microporosity of the Ni_3Al alloy treated with the DLMD and SLM processes.

In contrast, the parallel to scanning direction dendrites of the SLM processed samples are finer that of the DLMD one (fig. 6 c, d). The dendrites characteristic sizes were about 3 μm for the SLM samples and 5 μm for the DLMD samples. In fact, the structure refinement is directly connected with a cooling rate, i.e. a thermal gradient.

Apparently, the greater power density in case of the SLM processing (about six to ten times greater than the DLMD one) involves the greater thermal gradient. The last one is produced between environmental temperatures of the substrate bulk material and irradiated by the laser material. So the thermal gradient is directly depends on the temperature of surface irradiated by the laser beam, i.e. on the laser power density. In this regard, the thermal gradient depends on the scanning speed as well but, apparently, it plays a secondary role. Typically, the cooling rates of the DLMD process are about 10^4 - 10^5 K/s while the SLM one are about 10^6 K/s. In order to investigate the temperatures of a melting pool in the SLM and DLMD processes, additional researches should be carried out.

In-depth SEM study allows to precise that in general the microstructures are almost similar and depended of cooling rate i.e. process parameters. Fig. 7 of the SEM micrographs shows a slightly finer structure of the SLM produced sample. For the wide range of processing parameters, the microstructures are similar to the martensitic structure with fine 0.3-1.5 μm of width aciculas.

Figure 7 presents a little differences in gray scale that could originate from different elementary or a phase composition. Different phase's formation was provided by an element segregation that leads to the macro and micro liquation and no uniformity of strength properties.

As it shown at the fig. 6, 7, the macroporosity was not detected for the samples with optimal parameters as it is in the DLMD and SLM process parameters selection [18, 19]. Moving down of investigation scale allows discovering the micro porosity (fig. 8). Apparently, the reason of micro porosity is dissolved gases release because of the changing of solubility during a melting/solidification. The micropores characteristic size is 0.5…1 μm. In comparison with the nickel aluminide prepared with help of traditional casting, the SLM and DLMD present finer microstructures with microporosity finer of 5-10 times, as the cooling rate is greater [20].

3.3. Cracking

For both processes, the cracking did not occur during the single-tracks manufacturing. In contrast, for the multilayered samples the cracks were observed (fig. 9). The cracks have a tendency to the opening on application of a load (including a specimen cutting and grinding with high loads). The nickel aluminides alloys have a cracking susceptibility for a number of reasons and the hot and cold cracks could form [9]. The cracks have no regularity and propagate on the grain boundaries and through the grains.

The crack opening behavior is referred to the crack initiation on the solidification stage on the grain boundaries or in

the heat affected zone of adjacent tracks (underlayers). This indicates the high stresses in the solidification and

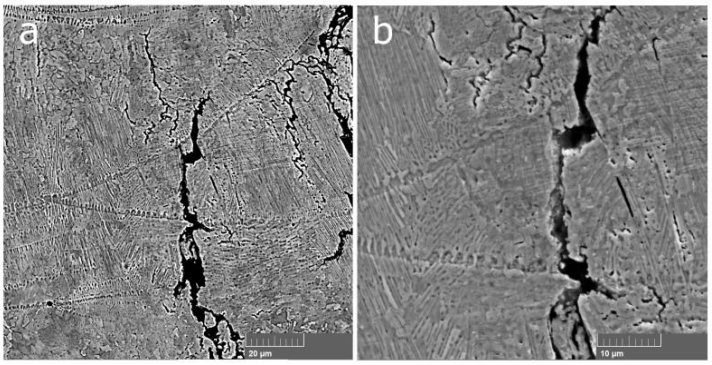

Figure 9. Cracks observed in the multilayered samples.

cooling zones as well as in the heat affected zone that provides origination and propagation of the cracks. The intermetallic nickel-aluminium alloys show an embrittlement at temperatures of 700-900 °C. In case of absence of alloy dopants that could reinforce the grain boundaries, the appropriate solution could be found in the thermal gradient decreasing with help, for example, of the working platform preheating to a 400-600 °C.

3.4. Elementary and Phase Composition

The SLM and DLMD samples were subjected to the EDX analysis in order to investigate the elementary composition of the processed material and homogeneity of elements distribution. The typical composition of material for both processes was 13…14% of aluminium and 86…87% of nickel that was corresponding to the initial intermetallic powder composition (fig. 10). The element distribution was uniform. For the SLM samples, the deviation in the element composition was detected in small areas with composition of about 68% of aluminium and 32% of nickel that could be attributed to the different from the Ni_3Al phase composition. Nevertheless, the large-scale analysis shows the typical element composition for both processes.

Figure 11 (a, b) shows the XRD pattern of the DLMD and SLM processed nickel aluminium material. Analysis of patterns presents almost similar phase composition with strong lines corresponded to the Ni_3Al phase and difference in minor phases. For the DLMD processed material a metastable Ni_2Al intermetallic phase occurs. While there was not detected the elementary difference the reason is that the Ni_2Al phase cell size could not be detected by relatively large electron beam in SEM study. The iron substrate is visible also as it may be supposed.

In contrast, the SLM processed material presents AlNi and alumina phase as the minor phases. The first one, apparently, was detected by the SEM EDX analysis (68Al 32Ni) that corresponds to the AlNi of Ni-Al phase diagram. Following the XRD pattern, the quantity of the AlNi phase is relatively low. Using the theory of metal matrix composite the AlNi phase could be as a strengthen element in more ductile Ni_3Al matrix. To investigate the influence of the AlNi phase content, the in-depth study is expected. The alumina Al_2O_3 phase is also detected regardless of the fact that the process was argon supported. The phase could also affect the elementary analysis. It should be note, that at the scanning velocities of 120 mm/s the minor phases have strongest lines than the one of 200 mm/s. The main result of the scanning velocity increasing is the more Ni_3Al phase contents. In addition, the SLM sample pattern presents smaller lines that could be attributed to the slightly finer structure. It should be note, that the relative content of Ni_3Al is more after SLM process, apparently, due to the stronger thermal cycle.

In comparison with the XRD pattern of initial powder, it is clear that the Ni_3Al phase lines directly corresponds to the XRD pattern of the DLMD and SLM material near the angles 30°, 40°, 50°, 60°, 90°, 110°. That means that, in general, both the DLMD and SLM processes allow transferring the powder phase composition to the structure of AM parts or repaired parts.

The crystal-lattice orientation of the γ'-Ni_3Al phase for both processes has a preferred direction of [111]. That is with particular attention could be taken into account that the equiaxed structure presents a higher creep strength than

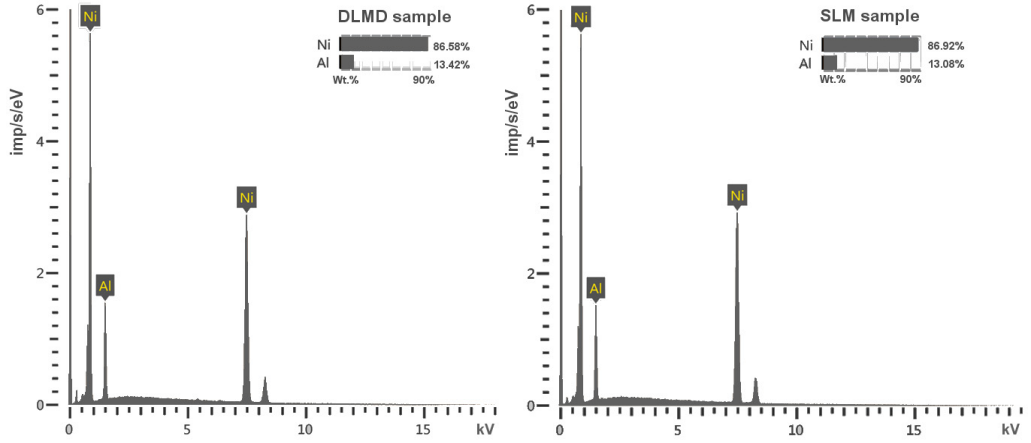

Figure 10. EDX pattern of the SLM (right) and the DLMD (left) samples.

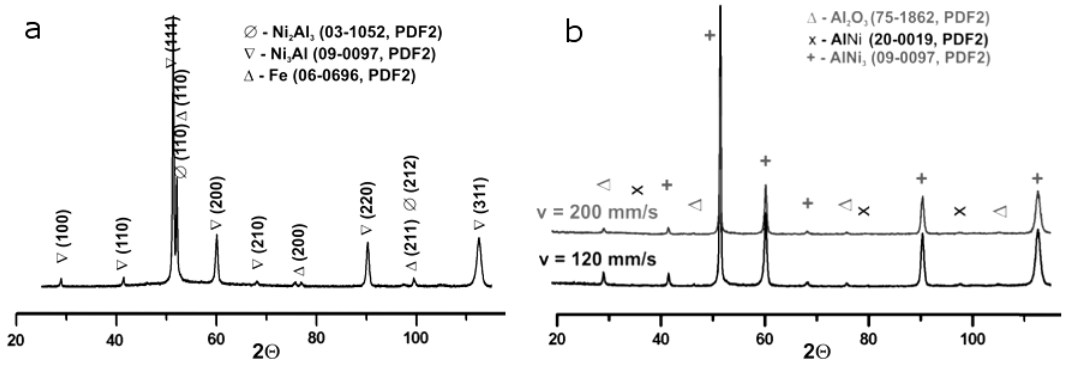

Figure 11. X-ray diffraction pattern of the DLMD (a) and the SLM (b) samples.

non-directional one [21].

4. Conclusion

Both processes show the manufacturability of the pre-alloyed Ni_3Al nickel aluminide powder. For the single tracks, layers and multilayered objects, several cross-sections with different geometries and structures were obtained. The geometry of the DLMD and SLM samples was in general similar with difference in minimum sizes of track cross-sections (200 μm and 70 μm, respectively). The SLM samples show smoother side view structure and the less rough surface. In contrast, the DLMD process allows belated in-flight particles to sinter with the surface. For both processes, the macrporosity was not detected, while the specimens presented microporosity with 0.5…1 μm sizes. Multilayered samples have the susceptibility to the cracking, apparently in the heat-affected zone because of strong thermal cycle.

The microstructure presents structures that are similar to the martensite for both processes. The dendrites were detected with the growing direction normal and parallel to the scanning direction. The SLM specimens present the finer structure because of different from the DLMD thermal cycle and the cooling rates.

General elementary composition presents almost uniform distribution of elements. The particular zones present

the deviation in element composition that was attributed to the different phase content. In this regard, the Ni_2Al and NiAl phases were detected for the DLMD and SLM processes, respectively.

Considering the scope of results and general knowledge, the DLMD and SLM processes have potential in the intended applications with various advantages and insufficiencies. Present study shows that there are no significant limitations in context of the material science between the DLMD and SLM processes. The future works shall be intended to highlight the parametric studies, thermal cycles and cooling rates as well as the strength tests with the different phase composition.

Acknowledgements

This work has been financed by the sources of the Russian Science Foundation (grant agreement №14-19-00992 from July 4, 2014).

References

1. D. Majumdar, I. Manna Laser material processing. *Int. Mater Rev* 2011;**56**(5-6):341-388.
2. I.Y. Smurov, A. Yakovlev Laser-Assisted Direct Manufacturing of Functionally Graded 3D Objects by Coaxial Powder Injection. *P Soc Photo-Opt Ins* 2004:27-37.
3. I. Yadroitsev, I. Smurov Selective Laser Melting Technology: from the Single Laser Melted Track Stability to 3D Parts of Complex Shape. *Phys Procedia* 2010;**5**:551-560.
4. A. Uriondo, M. Esperon-Miguez, S. Perinpanayagam The Present and Future of Additive Manufacturing in the Aerospace Sector: A Review of Important Aspects. *Proc Inst Mech Eng G J Aerosp Eng* 2015:1-16.
5. I. Yadroitsev, A. Gusarov, I. Yadroitsava & I. Smurov, Single Track Formation in Selective Laser Melting of Metal Powders. *J Mater Process Tech* 2010;**210***(*12):1624-1631.
6. D. Novichenko, A. Marants, L. Thivillon, P. H. Bertrand & I. Smurov, Metal Matrix Composite Material by Direct Metal Deposition. *Phys Procedia* 2011;**12**:296-302.
7. I.V. Shishkovsky Laser Controlled Intermetallics Synthesis during Surface Cladding In: [J. Lawrence et al.] *Laser Surface Engineering. Processes and applications*. Woodhead Publishing Series in Electronic and Optical Materials, Elsevier Science & Technology; Ch11, 2015, p. 237-286.
8. B.A. Grinberg, M.A. Ivanov *Intermetallidy Ni3Al i TiAl: Mikrostruktura, Deformatsionnoye Povedeniye*.[in the Russian] Yekaterinburg: UrO RAN, 2002 p. 360.
9. Zhu S. et al. Ni3Al Matrix High Temperature Self-Lubricating Composites. *Tribol Int* 2011;**44**(4):445-453.
10. Y. Yu; J. Zhou; Jianmin Chen J. et al.: Preparation, Microstructure and Tribological Behavior of Laser Cladding NiAl Intermetallic Compound Coatings. *Wear* 2012;**274–275**:298–305.
11. M. Duraiselvam et al. Cavitation Erosion Resistance of AISI 420 Martensitic Stainless Steel Laser-Clad with Nickel Aluminide Intermetallic Composites and Matrix Composites with TiC Reinforcement. *Surf Coat Technol*. 2006;**201**(3):1289-1295.
12. O. A. Bazyleva et al. Structure, Chemical Composition, and Phase Composition of Intermetallic Alloy VKNA-1V After High-Temperature Heat Treatment and Process Heating. *Met Sci Heat Treat* 2014; **56**(5-6): 229-234.
13. Cao G. et al. The Oxidation of Nanocrystalline Ni3Al Fabricated by Mechanical Alloying and Spark Plasma Sintering. *Intermetallics* 2007;**15**(12):1672-1677.
14. D. Kotoban, S. Grigoriev, I.Shishkovsky Study of 3D Laser Cladding for Ni85Al15 Superalloy. *Phys Procedia* 2014;**56**:262-268.
15. P. Podrabinnik, S. Grigoriev, I. Shishkovsky Laser Post Annealing of Cold-Sprayed Al/alumina–Ni Composite Coatings. *Surf Coat Technol* 2015;**271**:265–268.
16. I.V. Shishkovsky; A.G. Makarenko; A.L. Petrov: Conditions for SHS of Intermetallic Compounds with Selective Laser Sintering of Powdered Compositions. *Combust Explo Shock* 1999;**35**(2):166-170.
17. L. Zhang et al. Preparation and Properties of the Ni-Al/Fe-Al Intermetallics Composite Coating Produced by Plasma Cladding. *Int J Min Met Mater* 2011;**18**(6):725-730.
18. I. Smurov Laser Cladding and Laser Assisted Direct Manufacturing. *Surf Coat Technol* 2008;**202**(18):4496-4502.
19. I. Yadroitsev, P. Bertrand, I. Smurov Parametric Analysis of the Selective Laser Melting Process. *Appl Surf Sci* 2007;**253**(19):8064-8069.
20. S. C. Deevi and V. K. Sikk. Exo-Melt TM Process for Melting and Casting Intermetallics. *Intermetallics* 1997;**5**(1):17-27.
21. R. M. Nageswara Materials for Gas Turbines – An Overview In: [Ernesto B.] *Advances in Gas Turbine Technology*. Rieka, Croatia: InTech, 2011, p. 293-313